Received 5 October 2021; revised 20 December 2021; accepted 13 January 2022. Date of publication 15 March 2022; date of current version 22 March 2022.
The review of this article was arranged by Editor X. Guo.

Digital Object Identifier 10.1109/JEDS.2022.3157935

AM Mini-LED Backlight Driving Circuit Using PWM Method With Power-Saving Mechanism

CHIH-LUNG LIN [1,2] (Senior Member, IEEE), YI-CHIEN CHEN [1], JUI-HUNG CHANG [1], YU-SHENG LIN [3], SUNG-CHUN CHEN [1], MING-HSIEN LEE [4], AND CHUN-YEN CHANG [4]

1 Department of Electrical Engineering, National Cheng Kung University, Tainan 701-01, Taiwan
2 Advanced Optoelectronic Technology Center, National Cheng Kung University, Tainan 701-01, Taiwan
3 Electrical Engineering Department, Taipower Company, Kaohsiung 828107, Taiwan
4 Advanced Process Department, AU Optronics Corporation, Hsinchu 300-78, Taiwan

CORRESPONDING AUTHOR: C.-L. LIN (e-mail: cllin@ee.ncku.edu.tw)

This work was supported in part by the Advanced Optoelectronic Technology Center, National Cheng Kung University, Tainan, Taiwan; in part by the Ministry of Science and Technology of Taiwan under Project MOST 110-2221-E-006-149-MY3; and in part by the AU Optronics Corporation.

ABSTRACT This paper proposes a mini-light-emitting diode (mini-LED) driving circuit that is driven by pulse width modulation (PWM) for the backlights of active-matrix (AM) liquid crystal displays (LCDs). The proposed circuit compensates for threshold voltage (V_{TH}) variations of low-temperature poly-crystalline silicon thin-film transistors (LTPS TFTs) and the current-resistance (I-R) rise in VSS lines to supply a stable driving current. Operating the mini-LED at the high luminous efficacy by the PWM driving method and setting only the driving TFT on the path of the driving current reduce the power consumption of the backlight. Based on a 2.89-inch LCD panel with an AMLED 48 × 48 backlit module, the TFTs are fabricated, measured, and fitted. Simulation results show that the relative current error rates are all below 4.67% when the V_{TH} of the driving TFT varies by ±0.3 V and the VSS rises by 0.5 V. The voltage across VDD and VSS of the proposed circuit is 4.5 V lower than that of the 6T1C compensating driving circuit, so the power consumption of the circuit is at least 27.05% lower. Therefore, the proposed driving circuit is well suitable to use in mini-LED backlit LCDs.

INDEX TERMS Liquid crystal display (LCD), low-temperature poly-crystalline silicon (LTPS), mini-light-emitting diode (mini-LED), power consumption, pulse width modulation (PWM), threshold voltage (V_{TH}).

I. INTRODUCTION

The demand for high resolution displays with high contrast ratio has been increasing. Micro-light-emitting diodes (micro-LEDs) and mini-LEDs have attracted substantial attention due to their favorable characteristics, such as self-emission, high efficiency, long lifetime, and high brightness [1], [2]. However, the mass transfer technology for the manufacture of micro-LED displays is associated with numerous challenges because of its low yield and high cost. In contrast, since the complexity of fabrication decreases as the chip size of an LED increases, the fabrication of mini-LED is relatively mature [3]. Thus, the mini-LED, the fabrication of which has high yield, has been developed as a backlight unit in liquid-crystal displays (LCDs). For a mini-LED backlight, local dimming technology is utilized to improve the quality of images [3]–[5]. Since a mini-LED is smaller than a conventional LED, the number of dimming zones can be increased, improving the dynamic range and the contrast ratio of images. A mini-LED backlight is commonly driven by passive matrix (PM) or active matrix (AM) driving method. In the PM driving method, the resolution of the display is limited by the complexity of layout of the printed circuit board (PCB) and the patterning process on PCB substrates [5]. Also, the use of a large number of driver ICs to control these mini-LEDs increases the cost of the panel. However, with the AM driving method, the control signals for the gate on array (GOA) [6]–[8] and the input of data voltages can be provided by one driver IC [4], [9],

thus favoring a reduction in manufacturing costs. As such, the AM driving method is preferred.

To achieve high brightness of the mini-LED backlight for use in LCDs, the mini-LED must be driven at several milli-Ampere (mA) because of the low transmittance of the liquid crystal. Therefore, the low-temperature poly-crystalline silicon thin-film transistor (LTPS TFT) with high mobility and stable electrical characteristics is favored device to generate a high driving current for the mini-LED [10]–[12]. Nevertheless, the non-negligible threshold voltage (V_{TH}) variations of LTPS TFTs that are caused by the random distribution of grain boundaries in the channel leads to the generation of non-uniform driving currents by driving circuits [13]. Also, high driving currents induce dramatic current-resistance drop in the VSS and VDD power lines, severely distorting the driving currents [14]. Since the magnitude of the driving current is proportional to the luminance, these phenomena reduce the uniformity of the displayed luminance, degrading the quality of images. To reduce the influence of the VSS I-R rise, Liu *et al.* [15] presented a mini-LED backlight driving circuit that has four LEDs in series for each driving circuit to reduce the driving current to a quarter of that obtained using only one LED under the same luminance. The reduction in the driving current mitigates the effect of the VSS I-R rise but increases the cost of the display because it requires the use of numerous mini-LEDs. However, the V_{TH} variation of the TFT causes the generated driving currents in the pixels to be non-uniform. To solve the V_{TH} variation, several circuits with different compensating mechanisms have been reported [16]–[20]. Shin *et al.* [19] employed a diode-connected structure to compensate for the V_{TH} variation of the driving TFT, reducing the deviation in the emission current. Nevertheless, the additional switching TFTs on the path of the driving current increase the voltage across VDD and VSS because the flow of a current through a switching TFT generates the extra drain-to-source voltage (V_{DS}), increasing the static power consumption. Hence, Deng *et al.* [20] demonstrated a driving circuit that raises the V_{GS} of the switching TFT by the capacitive coupling method lowering its V_{DS} and thereby reduce power consumption. However, the reduced V_{DS} is still too high to greatly reduce the voltage between VDD and VSS. Furthermore, this circuit is driven by the pulse amplitude modulation (PAM) driving method, which controls gray levels by modifying the magnitude of the driving current. Hence, the operated luminous efficacy of the mini-LED varies with the driving currents. The luminous efficacy of a mini-LED is extremely low under low current, so the power consumption of the driving circuit that achieves the demanded luminance is increased. In contrast, the pulse width modulation (PWM) driving method generates a fixed current and adjusts the duty ratio of the emission time to control the gray level. Therefore, the mini-LED can be operated at high luminous efficacy [10], [21], so the power consumption of the backlight is reduced.

This work presents a new mini-LED backlight driving circuit using n-type LTPS TFTs. Using the PWM driving method to operate the mini-LED at high luminous efficacy and setting only one driving TFT on the path of the driving current minimize the voltage across VDD and VSS, reducing the power consumption of an LCD in which such mini-LEDs are used. Simulation results that are based on a 2.89-inch LCD panel with 2304 dimming zones establish the ability of the proposed circuit to generate uniform driving currents by compensating for both the V_{TH} variation of the driving TFT and the I-R rise of VSS. Relative to the previously developed 6T1C compensating circuit [22], the improvement of the power consumption of the proposed circuit at all gray levels is above 27.05%, revealing the feasibility of the power-saving mechanism.

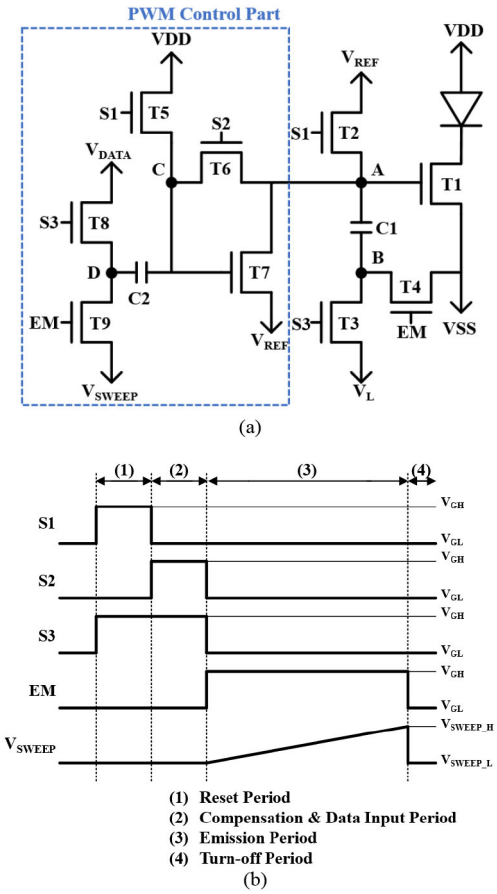

FIGURE 1. (a) Schematic and (b) timing diagram of proposed driving circuit.

II. OPERATION

Figs. 1(a) and 1(b) plot the schematic and timing diagram of the proposed driving circuit, which contains one driving TFT (T1), eight switching TFTs (T2-T9), and two capacitors (C1 and C2). Herein, T1 and T7 are matching TFTs with the same aspect ratio and electrical characteristics. The PWM control consists of five switching TFTs (T5-T9) and one capacitor (C2). S1, S2, S3, and EM are control signals that drive the switching TFTs. V_{SWEEP} is a sawtooth wave signal that activates T7 in a manner determined by the value of V_{DATA}.

The operation of the proposed driving circuit is divided into four periods, which are reset, compensation and data input, emission, and turn-off periods.

A. RESET PERIOD

S1 and S3 are high to turn on T2, T3, T5, and T8. S2 and EM are low to turn off T4, T6, and T9. Nodes B, C, and D are reset to V_L, VDD, and V_{DATA}, respectively. node A is discharged to V_{REF} by T2 and T7 to turn off T1. Therefore, T1 is turned off, preventing any current from flowing through the mini-LED.

B. COMPENSATION & DATA INPUT PERIOD

S1 goes low to turn off T2 and T5, and S2 goes high to turn T6 on. S3 remains high and keeps T8 on to deliver V_{DATA} to node D. T7 forms a diode-connected structure for V_{TH} compensation, so nodes A and C are discharged to $V_{REF} + V_{TH\_T7}$ until T7 is turned off where V_{TH_T7} is the threshold voltage of T7. The compensated voltages are stored in C1 and C2, and are given by the following equations.

$$V_{C1} = V_{REF} + V_{TH\_T7} - V_L \tag{1}$$

$$V_{C2} = V_{REF} + V_{TH\_T7} - V_{DATA} \tag{2}$$

where V_{C1} and V_{C2} are the voltages across the capacitors C1 and C2. Consistent with Eq. (1) and Eq. (2), the V_{TH} variation of T7 is sensed and can be used to compensate for V_{TH} variations in both driving and switching TFTs.

C. EMISSION PERIOD

S2 and S3 are switched low to turn off T3, T6, and T8, and EM switched high to turn on T4 and T9. node B is charged to VSS by T4 from V_L. Since node A is floating, the voltage of node A is boosted to $VSS - V_L + V_{REF} + V_{TH\_T7}$ based on the charge conservation of C1. T1 is turned on to generate the driving current as follows.

$$\begin{aligned} I_{LED} &= \frac{1}{2}k\left(V_{GS\_T1} - V_{TH\_T1}\right)^2 \\ &= \frac{1}{2}k\left(VSS - V_L + V_{REF} + V_{TH\_T7} - VSS - V_{TH\_T1}\right)^2 \\ &= \frac{1}{2}k(V_{REF} - V_L)^2 \end{aligned} \tag{3}$$

where k is $\mu \cdot C_{ox} \cdot W/L$ of T1 and I_{LED} is mini-LED current. The V_{TH} variation of T1 is compensated for by the matching TFT method since T1 and T7 are matching TFTs. The capacitive coupling method is used to couple the voltage of VSS to the gate node of the driving TFT through C1, which compensates for the VSS I-R rise. Eq. (3) is obtained by eliminating V_{TH_T1} and VSS from the equation for I_{LED}, so the V_{TH} variation of the driving TFT and the rise of VSS do not influence the uniformity of the driving current. For the PWM control, node D is firstly discharged to V_{SWEEP_L} by T9, and node C is coupled to $V_{SWEEP\_L} - V_{DATA} + V_{REF} + V_{TH\_T7}$ by C2. Since V_{SWEEP} is a sawtooth wave, the voltage of node D gradually increases, and C2 couples the voltage differences of node D to the floating node C. As the voltage of node C continuously increases, T7 will be turned on in the following condition.

$$\begin{aligned} V_{GS\_T7} &= V_{G\_T7} - V_{S\_T7} > V_{TH\_T7} \\ &\Rightarrow \left(V_{SWEEP} - V_{DATA} + V_{REF} + V_{TH\_T7}\right) \\ &\quad - V_{REF} > V_{TH\_T7} \\ &\Rightarrow V_{SWEEP} > V_{DATA} \end{aligned} \tag{4}$$

According to Eq. (4), when V_{SWEEP} is larger than V_{DATA}, T7 is turned on and discharges node A to V_{REF} to turn T1 off. Since the V_{TH} variation of T7 is compensated for by the diode-connected structure of T7, the total emission time depends only on the value of V_{DATA} and is unaffected by the V_{TH} variation of T7.

D. TURN-OFF PERIOD

S1, S2, S3, and EM are low to turn off all TFTs. node A is maintained at V_{REF}, keeping T1 off to avoid the flow of any current through the mini-LED and to prevent the backlight from flickering.

The proposed circuit adopts the active driving method in which the emission of light occurs only in the emission period, whereas black images are generated in the other periods. By inserting a long period of black images which accounts for 92.8% of a frame time and simultaneously lighting mini-LEDs in the same row, the effect of the pseudo contour phenomenon on moving images is reduced.

In the aforementioned operation, the proposed circuit compensates for the V_{TH} variation of the driving TFT and the I-R rise of VSS to produce uniform and fixed driving currents, enabling the mini-LED to be maintained at high luminous efficacy. With respect to the PWM control, after the V_{TH} variation of T7 has been compensated for, the condition under which the emission time is controlled is independent of the V_{TH} variation of T7. Furthermore, the mini-LEDs are turned off except in the emission period to generate high-contrast-ratio images. Therefore, the proposed circuit generates uniform driving currents and increases the quality of black images.

III. RESULTS AND DISCUSSION

To investigate the effectiveness of the proposed mini-LED backlight driving circuit, the electrical characteristics of the fabricated LTPS TFTs are measured to establish TFT models using the HSPICE simulator with the Level 62 RPI poly-silicon TFT model. Figs. 2(a) and 2(b) plot the current-to-voltage (I-V) characteristics of a driving TFT with an aspect ratio of 1040 μm/(7 + 7) μm and a switching TFT with an aspect ratio of 6 μm/(3+3) μm, respectively, when V_{GS} ranges from −15 V to 15 V. Fig. 3(a) plots the I-V characteristic of the mini-LED. A 2.63 V of forward voltage is generated when 2 mA of driving current flowing through the mini-LED. Fig. 3(b) presents a layout image of the proposed circuit, of which the area is 1000 μm × 1000 μm. Notably, the resistance of VSS is reduced to ameliorate the VSS I-R

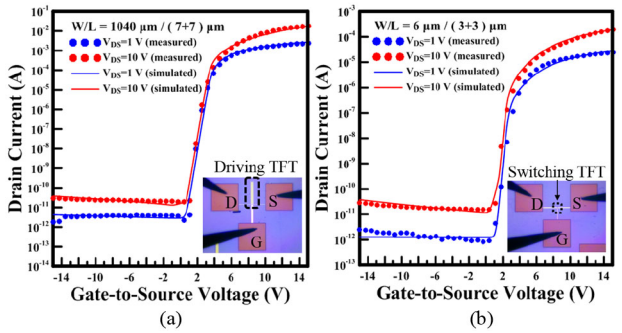

FIGURE 2. Measured and fitted I_D-V_{GS} curves of (a) driving and (b) switching TFTs at V_{DS} = 1 V and 10 V.

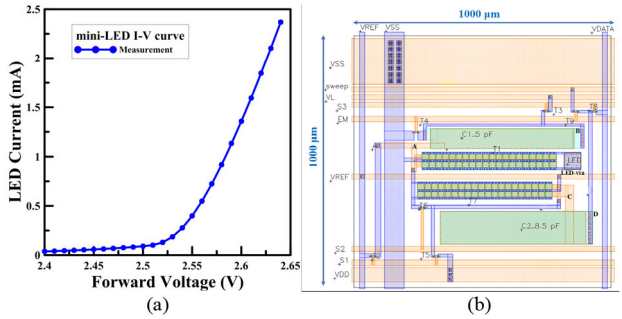

FIGURE 3. (a) Measured I-V characteristic of mini-LED. (b) Layout image of single backlight unit.

TABLE 1. Parameters of proposed driving circuit.

TFT Aspect Ratio and Capacitance			
T1, T7 (μm/μm)	1040 / (7+7)	C1 (pF)	5
T2-T6 (μm/μm)	6 / (3+3)	C2 (pF)	8.5
T8, T9 (μm/μm)	6 / (3+3)		
Voltages of Signals			
S1-S3, EM (V)	-6 ~ 13	VDD (V)	9.5
V_L (V)	-5.8	VSS (V)	-1
V_{DATA} (V)	0 ~ 7	V_{REF} (V)	-1
V_{SWEEP} (V)	1 ~ 8.5		

rise by adding a metal layer as a power metal mesh [5]. Table 1 lists the channel length and width of the TFTs, the capacitance of the capacitors, and the voltage swing of the signal lines in the proposed circuit. Herein, all design parameters are based on the specifications of a mini-LED backlight module that has 2304 local dimming zones, a frame rate of 90 Hz, and a total gray level of 64 for use in a 2.89-inch LCD panel. The driving current of the proposed circuit is up to 2 mA, and the maximum emission time is 805 μs, yielding a maximum luminance of 14,000 nits, used for backlights in virtual reality (VR) LCDs.

Fig. 4 shows the transient waveforms of the I_{LED}, and the voltage of the gate nodes of the driving and switching TFTs, with VSS I-R rises of 0.5 V and V_{TH} variations of ±0.3 V. According to Fig. 4(a), at the end of the compensation period,

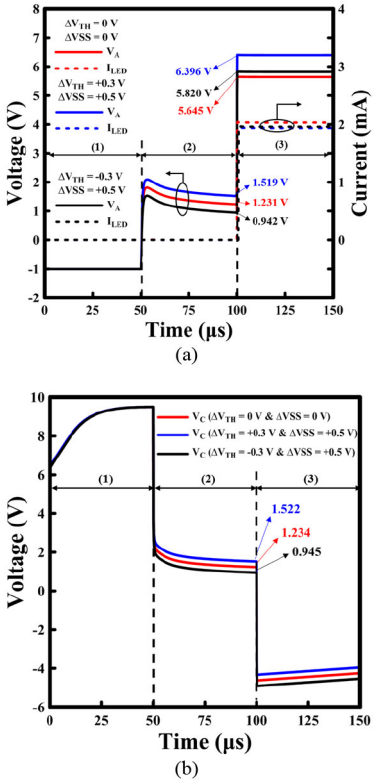

FIGURE 4. Simulated transient waveforms with V_{TH} variations of ±0.3 V and VSS I-R rise of 0.5 V for (a) node A, I_{LED}, and (b) node C.

the voltages of node A are discharged to 1.519 V, 1.231 V, and 0.942 V, respectively, so namely the proposed circuit senses the V_{TH} variation of 0.288 V and −0.289 V. During the emission period, the voltages of node A are boosted to 6.396 V, 5.820 V, and 5.645 V, demonstrating that the V_{TH} variation and the VSS I-R rise are compensated for by the matching TFT method and the capacitive coupling method, respectively. Furthermore, no unexpected current flows through the mini-LED during the reset period, and the compensation and data input period, increasing the contrast ratio of the panel. As shown in Fig. 4(b), the diode-connected structure of T7 detects V_{TH} variation of T7 of 0.288 V and −0.289 V in a compensation period of 50 μs. Since the sensed V_{TH} of T7 is stored in C2, the condition that activates T7 is immune to V_{TH} variation. Thus, the emission time of the proposed circuit is independent of the V_{TH} variation of T7.

Fig. 5(a) compares driving currents of the proposed circuit with those of the conventional 2T1C circuit at different gray levels for a VSS I-R rise of 0.5 V and a V_{TH} variation of the driving TFT of ±0.3 V. For the proposed circuit with the PWM driving method, driving currents at all gray levels are around 2 mA, showing the effectiveness of the matching TFT method and the capacitive coupling method to compensate for the V_{TH} variation of the driving TFT and the VSS I-R rise. In contrast, the 2T1C driving circuit with no compensating mechanism suffers from the V_{TH} variation

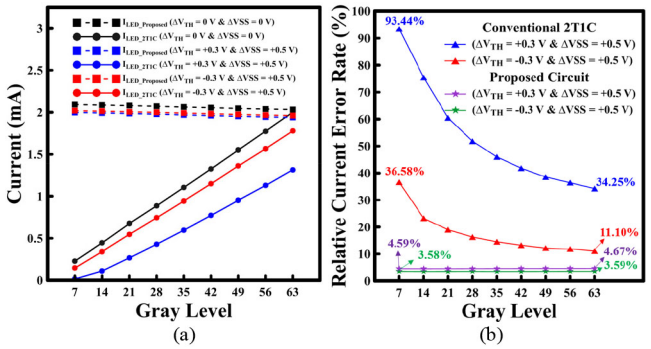

FIGURE 5. Comparison of (a) driving currents and (b) relative current error rates at different gray levels of conventional 2T1C circuit and proposed circuit with V_{TH} variations of driving TFT of ±0.3 V and VSS I-R rise of 0.5 V.

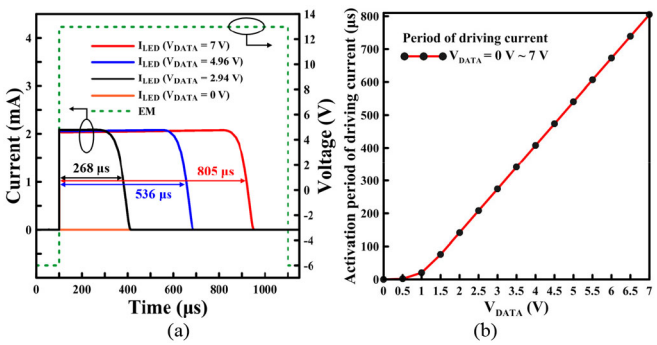

FIGURE 6. (a) Transient waveforms of I_{LED} at high, medium, low, and zero gray level. (b) Relationship between V_{DATA} and activation period of driving current.

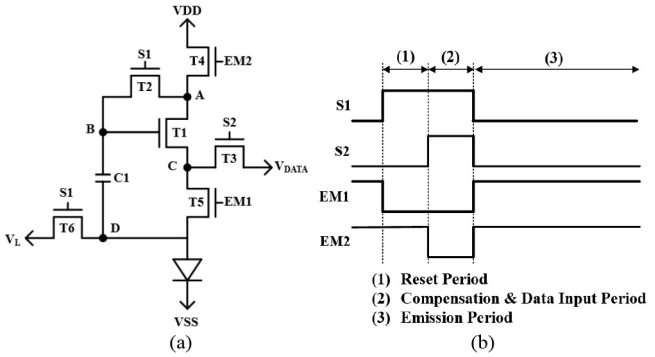

FIGURE 7. (a) Schematic and (b) timing diagram of previously developed 6T1C circuit [22].

TABLE 2. Parameters of previously developed 6T1C circuit.

TFT Aspect Ratio and Capacitance			
T1, T4, T5 (μm/μm)	1040 / (7+7)	C1 (pF)	5
T2, T3, T6 (μm/μm)	6 / (3+3)		
Voltages of Signals			
S1, S2 (V)	-6 ~ 13	VDD (V)	9.5
EM1, EM2 (V)	-6 ~ 13	VSS (V)	-5.5
V_{DATA} (V)	-5.8 ~ -0.3	V_L (V)	-5.8

of the driving TFT and the I-R rise of VSS, causing non-uniformity in the driving current. Thus, the driving currents of the proposed circuit are more uniform than those of the conventional 2T1C circuit. Fig. 5(b) shows the relative current error rates of both circuits at different gray levels. The relative current error rates of the 2T1C circuit range from 11.10% to 93.44% while those of the proposed circuit are all below 4.67%, revealing that the driving currents of the proposed circuit are more uniform.

To confirm the ability of the proposed PWM method to control the gray level, Fig. 6(a) shows driving currents with four values of V_{DATA} to modify the emission time of the mini-LED at different gray levels. When V_{DATA} is set to 7 V, 4.96 V, 2.94 V, and 0 V, the emission times are 805 μs, 536 μs, 268 μs, and 0 μs representing the high, medium, low, and zero gray levels, respectively. Fig. 6(b) plots the relationship between V_{DATA} and the activation period of driving currents, which is the emission time of the mini-LED. When V_{DATA} ranges from 1.5 V to 7 V, the relationship is linear because the falling times of the driving currents within this data voltage range are equal, so a long falling time does not affect the linearity between V_{DATA} and the activation period of the driving current. With V_{DATA} in the range from 0 V to 1.5 V, a non-linear relationship obtains at low gray levels. However, a wide data voltage range is employed to determine a few gray levels, so these gray levels can be differentiated more finely to increase the controllability of these low gray levels of the mini-LED backlight. Therefore, modifying the activation period of the driving current by using different V_{DATA} confirms the linearity of the relationships between the currents and data voltages of the proposed circuit.

To investigate the effectiveness of the power-saving mechanism in the proposed circuit, the power consumption of the proposed circuit is compared with that of the previously developed 6T1C compensating circuit [22]. Fig. 7(a) shows the structure of the 6T1C compensating circuit, and Fig. 7(b) displays the timing diagram of the control signals. For a fair comparison, the parameters of the proposed circuit and the previously developed 6T1C circuit are based on the same specifications. The design parameters of the 6T1C circuit are shown in Table 2. Figs. 8(a) and 8(b) plot the voltages of the nodes on the driving current path of the proposed circuit and the previously developed 6T1C circuit. For a maximum gray level of 63, the V_{GS} and V_{DS} of the driving TFT in both circuits are equivalent to 6.64 V and 7.87 V to generate driving currents of the same magnitude. The voltage across VDD and VSS in the proposed circuit is 10.5 V to generate the driving current of 2 mA. In contrast, the voltage across VDD and VSS in the 6T1C circuit is 4.5 V higher because a driving current of 2 mA flowing through the two extra switching TFTs generates a V_{DS} of 3.78 V in T4 and a V_{DS} of 0.72 V in T5. Hence, the total voltage across VDD and VSS of the 6T1C circuit is 15 V, which increases the static power consumption of the circuit. The improvement of the static power consumption of the

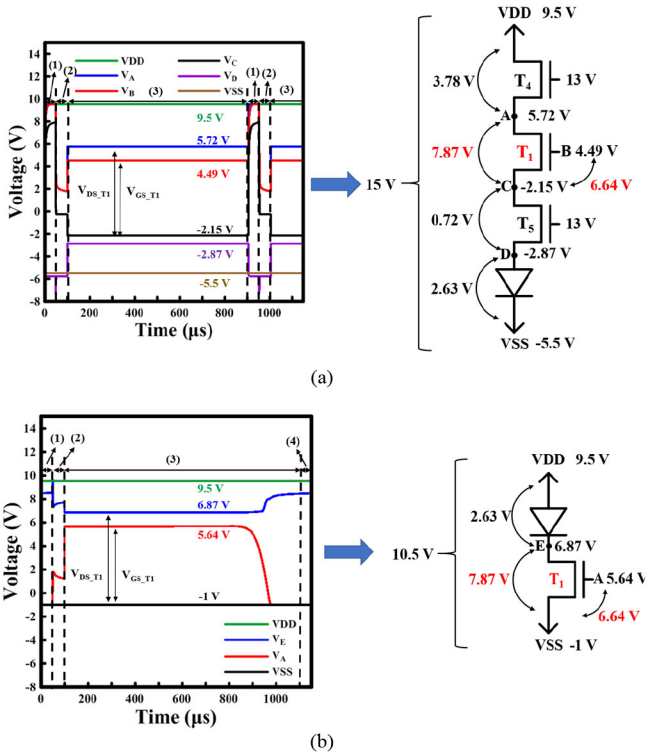

FIGURE 8. **Transient waveforms of all nodes on driving current path for (a) previously developed 6T1C and (b) proposed circuit at gray level of 63.**

TABLE 3. **Power consumption of proposed and previously developed 6T1C circuit and corresponding improvement.**

Power Consumption			Improvement (%)
Gray Level	Proposed circuit (mW)	6T1C circuit (mW)	
7	0.177	0.248	28.60
14	0.353	0.484	27.05
21	0.527	0.734	28.10
28	0.701	0.964	27.33
35	0.872	1.201	27.40
42	1.042	1.441	27.68
49	1.211	1.684	28.13
56	1.379	1.929	28.52
63	1.547	2.174	28.85

proposed circuit over that of the 6T1C circuit is calculated as follows.

$$\text{Improvement } (\%) = \frac{P_{\text{Static}-6T1C} - P_{\text{Static}-\text{Proposed}}}{P_{\text{Static}-6T1C}} \times 100\%$$

where $P_{\text{Static-Proposed}}$ and $P_{\text{Static-6T1C}}$ are the static power consumption of the proposed circuit and that of the 6T1C circuit, respectively. Table 3 compares the power consumption of the 6T1C circuit with that of the proposed circuit. The power consumption of the proposed circuit at each gray level is lower than that of the 6T1C circuit, and the improvement of the power consumption at all gray levels is above 27.05%, demonstrating that placing only one driving TFT on the path of the driving current saves power. Therefore, the power-saving method makes the proposed mini-LED backlight circuit suitable for use in VR LCDs.

IV. CONCLUSION

This work proposes a mini-LED driving circuit to produce a stable driving current by compensating for the I-R rise of VSS and the V_{TH} variation of the driving TFT. By using the PWM driving method, the proposed circuit operates the mini-LED at the high luminous efficacy to save the power of the backlight. Furthermore, setting only one TFT on the driving current path further reduces the power consumption of the backlight. Simulation results show that the proposed circuit generates uniform driving current with a current error rate below 4.67% when the VSS rises by 0.5 V and the V_{TH} of the driving TFT varies by ±0.3 V. The voltage across VDD and VSS for the proposed circuit is reduced by a voltage of 4.5 V lower than that in the 6T1C circuit, so the maximum improvement of 28.85% in power consumption is achieved. Therefore, the proposed mini-LED driving circuit is promising for use in the backlight of VR LCDs.

REFERENCES

[1] Z. J. Liu, W. C. Chong, K. M. Wong, K. H. Tam, and K. M. Lau, "A novel BLU-free full-color LED projector using LED on silicon micro-displays," *IEEE Photon. Technol. Lett.*, vol. 25, no. 23, pp. 2267–2270, Dec. 1, 2013.

[2] J. Oh *et al.*, "Pixel circuit with P-type low-temperature polycrystalline silicon thin-film transistor for micro light-emitting diode displays using pulse width modulation," *IEEE Electron Device Lett.*, vol. 42, no. 10, pp. 1496–1499, Oct. 2021.

[3] T. Wu *et al.*, "Mini-LED and micro-LED: Promising candidates for the next generation display technology," *Appl. Sci.*, vol. 8, p. 1557, Sep. 2018.

[4] Y. Huang, G. Tan, F. Gou, M. C. Li, S. L. Lee, and S. T. Wu, "Mini-LED enhanced LCD for high dynamic range displays," in *SID Symp. Dig. Tech. Papers*, vol. 50, May 2019, pp. 569–572.

[5] Y.-E. Wu, M.-H. Lee, Y.-C. Lin, C. Kuo, Y.-H. Lin, and W.-M. Huang, "41–1: Invited Paper: Active matrix mini-LED backlights for 1000PPI VR LCD," in *SID Symp. Dig. Tech. Papers*, vol. 50, May 2019, pp. 562–565.

[6] C.-L. Lin, M.-Y. Deng, C.-E. Wu, C.-C. Hsu, and C.-L. Lee, "Hydrogenated amorphous silicon gate driver with low leakage for thin-film transistor liquid crystal display applications," *IEEE Trans. Electron Devices*, vol. 64, no. 8, pp. 3193–3198, Aug. 2017.

[7] C.-L. Lin, C.-E. Wu, F.-H. Chen, P.-C. Lai, and M.-H. Cheng, "Highly reliable bidirectional a-InGaZnO thin-film transistor gate driver circuit for high-resolution displays," *IEEE Trans. Electron Devices*, vol. 63, no. 6, pp. 2405–2411, Jun. 2016.

[8] H. J. Shin and T. W. Kim, "Ultra-high-image-density, large-size organic light-emitting device panels based on highly reliable gate driver circuits integrated by using InGaZnO thin-film transistors," *IEEE J. Electron Devices Soc.*, vol. 7, pp. 1109–1113, 2019.

[9] J. Xiao *et al.*, "Mini-LED backlight units on glass for 75-inch 8K resolution liquid crystal display," *J. Soc. Inf. Display*, vol. 30, pp. 54–60, May 2021.

[10] C.-L. Lin *et al.*, "AM PWM driving circuit for mini-LED backlight in liquid crystal displays," *IEEE J. Electron Devices Soc.*, vol. 9, pp. 365–372, 2021.

[11] C.-L. Lin, C.-C. Hung, P.-Y. Kuo, and M.-H. Cheng, "New LTPS pixel circuit with AC driving method to reduce OLED degradation for 3D AMOLED displays," *J. Display Technol.*, vol. 8, no. 12, pp. 681–683, Dec. 2012.

[12] S.-C. Chen *et al.*, "Nonvolatile polycrystalline silicon thin-film-transistor memory with oxide/nitride/oxide stack gate dielectrics and nanowire channels," *Appl. Phys. Lett.*, vol. 90, Mar. 2007, Art. no. 122111.

[13] T.-F. Chen, C.-F. Yeh, and J.-C. Lou, "Investigation of grain boundary control in the drain junction on laser-crystalized poly-Si thin film transistors," *IEEE Electron Device Lett.*, vol. 24, no. 7, pp. 457–459, Jul. 2003.
[14] Y.-C. Lin and H.-P. D. Shieh, "Improvement of brightness uniformity by AC driving scheme for AMOLED display," *IEEE Electron Device Lett.*, vol. 25, no. 11, pp. 728–730, Nov. 2004.
[15] B. Liu *et al.*, "An active matrix mini-LEDs backlight based on a-Si," in *SID Symp. Dig. Tech. Papers*, vol. 51, Jul. 2020, pp. 62–64.
[16] Y. Kim, Y. Kim, and H. Lee, "A novel a-InGaZnO TFT pixel circuit for AMOLED display with the enhanced reliability and aperture ratio," *J. Display Tech.*, vol. 10, no. 1, pp. 80–83, Jan. 2014.
[17] R. M. A. Dawson *et al.*, "The impact of the transient response of organic light emitting diodes on the design of active matrix OLED displays," in *IEDM Tech. Dig.*, San Francisco, CA, USA, 1998, pp. 875–878.
[18] H.-J. In and O.-K. Kwon, "External compensation of nonuniform electrical characteristics of thin-film transistors and degradation of OLED devices in AMOLED displays," *IEEE Electron Device Lett.*, vol. 30, no. 4, pp. 377–379, Apr. 2009.
[19] W.-S. Shin *et al.*, "A driving method of pixel circuit using a-IGZO TFT for suppression of threshold voltage shift in AMLED displays," *IEEE Electron Device Lett.*, vol. 38, no. 6, pp. 760–762, Jun. 2017.
[20] M.-Y. Deng *et al.*, "Reducing power consumption of active-matrix mini-LED backlit LCDs by driving circuit," *IEEE Trans. Electron Devices*, vol. 68, no. 5, pp. 2347–2354, May 2021.
[21] M. Kimura, D. Suzuki, M. Koike, S. Sawamura, and M. Kato, "Pulsewidth modulation with current uniformization for AM-OLEDs," *IEEE Trans. Electron Devices*, vol. 57, no. 10, pp. 2624–2630, Oct. 2010.
[22] T. K. Chang, C. W. Lin, and S. Chang, "39-3: Invited Paper: LTPO TFT technology for AMOLEDs," in *SID Symp. Dig. Tech. Papers*, vol. 50, May 2019, pp. 545–548.

CHIH-LUNG LIN (Senior Member, IEEE) received the M.S. and Ph.D. degrees in electrical engineering from National Taiwan University, Taipei, Taiwan, in 1993 and 1999, respectively. He is currently a Professor with the Department of Electrical Engineering, National Cheng Kung University, Tainan, Taiwan. His current research interests include pixel circuits design for AMOLEDs, gate driver circuit design for AMLCDs, and flexible display circuits.

YI-CHIEN CHEN received the B.S. degree in electrical engineering from National Central University, Taoyuan, Taiwan, in 2020. He is currently pursuing the M.S. degree in electrical engineering with National Cheng Kung University, Tainan, Taiwan. His research focuses on the system circuit design for mini-LED and AMOLED displays.

JUI-HUNG CHANG received the B.S. degree in electrical engineering from National Central University, Taoyuan, Taiwan, in 2017, and the M.S. degree in electrical engineering from National Cheng Kung University, Tainan, Taiwan, in 2019, where he is currently pursuing the Ph.D. degree in electrical engineering. His research focuses on gate driver circuit design on glass for AMLCD and pixel circuit design for AMOLED.

YU-SHENG LIN received the B.S. and M.S. degrees in electrical engineering from National Cheng Kung University, Tainan, Taiwan, in 2017 and 2019, respectively. He is currently an Engineer with the Taipower Company, Kaohsiung, Taiwan.

SUNG-CHUN CHEN received the B.S. degree in electrical engineering from National Cheng Kung University, Tainan, Taiwan, in 2019, where he is currently pursuing the Ph.D. degree in electrical engineering. His research focuses on the system circuit design for mini-LED and AMOLED displays.

MING-HSIEN LEE received the B.S. and Ph.D. degrees in electrical engineering from National Chiao-Tung University, Hsinchu, Taiwan, in 2000 and 2007, respectively. He is currently a Manager and a Principle Researcher with the AU Optronics Corporation, Hsinchu. His recent research interests include micro-LED and mini-LED backplane technologies, serving for public information displays and VR applications.

CHUN-YEN CHANG received the B.S. and M.S. degrees in electrical engineering from the National Kaohsiung University of Applied Sciences, Kaohsiung, Taiwan, in 2015 and 2017, respectively. He is currently a Senior Engineer with the AU Optronics Corporation, Hsinchu, Taiwan.